**Steel and Composite Structures**, *Vol. 23, No. 5 (2017) 597-610*
DOI: https://doi.org/10.12989/scs.2017.23.5.597


# Modeling for fixed-end moments of I-sections with straight haunches under concentrated load

Inocencio Luévanos Soto [a] and Arnulfo Luévanos Rojas*

*Faculty of Engineering, Science and Architecture, Juárez University of Durango State, Av. Universidad S/N, Fracc. Filadelfia, CP 35010, Gómez Palacio, Durango, México*

(*Received June 25, 2015, Revised December 04, 2016, Accepted February 10, 2017*)

**Abstract.** This paper presents a mathematical model for fixed-end moments of I-sections with straight haunches for the general case (symmetrical and/or non-symmetrical) subjected to a concentrated load localized anywhere on beam taking into account the bending deformations and shear, which is the novelty of this research. The properties of the cross section of the beam vary along its axis "*x*", i.e., the flange width "*b*", the flange thickness "*t*", the web thickness "*e*" are constant and the height "*d*" varies along of the beam, this variation is linear type. The compatibility equations and equilibrium are used to solve such problems, and the deformations anywhere of beam are found by the virtual work principle through exact integrations using the software "Derive" to obtain some results. The traditional model takes into account only bending deformations, and others authors present tables considering the bending deformations and shear, but are restricted. A comparison between the traditional model and the proposed model is made to observe differences, and an example of structural analysis of a continuous highway bridge under live load is resolved. Besides the effectiveness and accuracy of the developed models, a significant advantage is that fixed-end moments are calculated for any cross section of the beam "I" using the mathematical formulas.

**Keywords:** fixed-end moments; beams of I-sections; concentrated load; straight haunches; bending deformations and shear

## 1. Introduction

Beams with haunches of "I-sections" found its application in buildings and bridges of various functions. In buildings, nonprismatic structural members with stepped haunches, straight or parabolic, which is applied commonly in engineering design to reduce weight and optimize the strength and stability or to meet architectural requirements and specifics functional. On the bridges the live load corresponds to concentrated loads transmitted by the vehicles through their wheels to the road surface on the board.

In structural engineering there are circumstances, where the beams are non-uniform, in the sense of the geometry and/or material properties varying along length. One of the main problems in the analysis of structures with moment of inertia variable along its length is obtain the fixed-end moments, stiffness, and carry-over factors.

To middle of last century were developed several design aids, as those presented by Guldan (1956), and most know tables published by the Portland Cement Association (PCA), where stiffness constants and fixed-end moments of variable section members are presented (Portland Cement Association 1958). Hypotheses used to simplify the problem are: (1) the variation of the stiffness (linear or parabolic, according the case of geometry) in function of main moment of inertia in bending; (2) the shear deformations and the ratio of length-height of beam are neglected in the definition of several stiffness factors (Tena-Colunga 1996).

After the publication of the PCA tables, the following works deserve special mention based on beams theory. Just (1977) was the first to propose the formulation to bending, and the axial stiffness matrix for beams of tapering box and I-section. Schreyer (1978) developed, with the use of a generalized Kirchhoff hypothesis in which the transverse shear strain in cylindrical coordinates is assumed to be zero; a beam theory is developed for linearly tapered members. Medwadowski (1984) presented a solution of the problem of bending of nonprismatic beams, including the effect of shear deformations. Brown (1984) proposed a method to find a modified bending stiffness matrix for tapered beams. Matrix of elastic stiffness for two-dimensional and three-dimensional members of variable section based on classical theory of beam by Euler-Bernoulli and flexibilities method taking into account the axial and shear deformations, and the cross section shape is found in Tena-Colunga and Zaldo (1994) and in the appendix B (Tena-Colunga 2007). But the tables are limited to certain relationships, and also the heights of the haunches are the same at both ends.

Recently published papers are: Yuksel (2009) this study aimed to investigate the modeling, analysis and behavior of the non-prismatic members subjected to temperature changes. Shooshtari and Khajavi (2010) proposed to find the shape functions and stiffness matrices of nonprismatic

*Corresponding author, Ph.D.,
E-mail: arnulfol_2007@hotmail.com
[a] Ph.D. Candidate, E-mail: arq_inothrain@hotmail.com


http://www.techno-press.org/?journal=scs&subpage=6 ISSN: 1229-9367 (Print), 1598-6233 (Online)

beam elements. Yuksel (2012) realized a study aimed to investigate the behavior of non-prismatic beams with symmetrical parabolic haunches (NBSPH) having the constant haunch length ratio of 0.5. Fiore *et al*. (2012) show a viscoelastic behaviour of non-homogeneous variable-section beams with post-poned restraints. Won *et al*. (2012) presented the forced vibration analysis of damped beam structures with composite cross-section using Timoshenko beam element. Cristutiu *et al*. (2012) show an experimental study on laterally restrained steel columns with variable I cross sections. Saffari *et al*. (2012) presented a free vibration analysis of non-prismatic beams under variable axial forces. Luévanos-Rojas (2013c) proposed a mathematical model for rectangular beams of variable cross section of symmetrical parabolic shape for uniformly distributed load. Luévanos-Rojas and Montoya-Ramirez (2014) presented a mathematical model for rectangular beams of variable cross section of symmetrical linear shape for uniformly distributed load. Huang *et al*. (2014) presented the power spectra of wind forces on a high-rise building with section varying along height. Luévanos-Rojas *et al*. (2014) proposed a mathematical model for rectangular beams of variable cross section of symmetrical linear shape for concentrated load. Luévanos-Rojas (2014) presented a mathematical model for fixed-end moments for two types of loads for a parabolic shaped variable rectangular cross section. Albegmprli *et al*. (2015) show the reliability analysis of reinforced concrete haunched beams shear capacity based on stochastic nonlinear FE analysis. Luévanos-Rojas (2015) proposed a modeling for beams of "I" cross-section subjected to a uniformly distributed load with straight haunches taking into account the bending deformations and shear to obtain the fixed-end moments, carry-over factors and stiffness factors.

Traditional methods used for the variable cross section members, the deflections are obtained by Simpson's rule or some other technique to perform numerical integration, and tables presenting some books are limited to certain relationships, and also shear deformations are not considered (Hibbeler 2006, Vaidyanathan and Perumal 2006, Williams 2008).

This paper presents a mathematical model for fixed-end moments of I-sections with straight haunches for the general case (symmetrical and/or non-symmetrical) subjected to a concentrated load localized anywhere on beam taking into account the bending deformations and shear, which is the novelty of this research. The properties of the cross section of the beam vary along its axis "$x$", i.e., the flange width "$b$", the flange thickness "$t$", the web thickness "$e$" are constant and the height "$d$" varies along the beam, this variation is linear type. The compatibility equations and equilibrium are used to solve such problems, and the deformations anywhere of beam are found by means of the virtual work principle through exact integrations using the software "Derive" to obtain some results. The traditional model takes into account only bending deformations, and others authors present tables considering the bending deformations and shear, but are restricted. A comparison between the traditional model and the proposed model is made to observe differences, and an example of structural analysis of a continuous highway bridge under live load is resolved.

## 2. Formulation the mathematical model

### *2.1 Properties of the "I" cross-section*

Fig. 1 shows a beam in elevation and also presents its "I" cross-section taking into account the flange width "$b$", the flange thickness "$t$", the web thickness "$e$" are constant, and the height "$d$" varies along the beam, this variation is linear type in three different parts.

Equations of the web height "$d_y$" shear area "$A_{sx}$" and the moment of inertia around the axis Z "$I_z$" to a distance "$x$" for each segment are (Luévanos-Rojas 2015)

To $0 \le x \le a$

$$d_{y1} = \frac{ad + u(a-x)}{a} \tag{1}$$

$$A_{sx1} = e\left[\frac{ad + u(a-x) + 2at}{a}\right] \tag{2}$$

$$I_{z1} = \frac{b[ad + u(a-x) + 2at]^3 - (b-e)[ad + u(a-x)]^3}{12a^3} \tag{3}$$

To $a \le x \le L - c$

$$d_{y2} = d \tag{4}$$

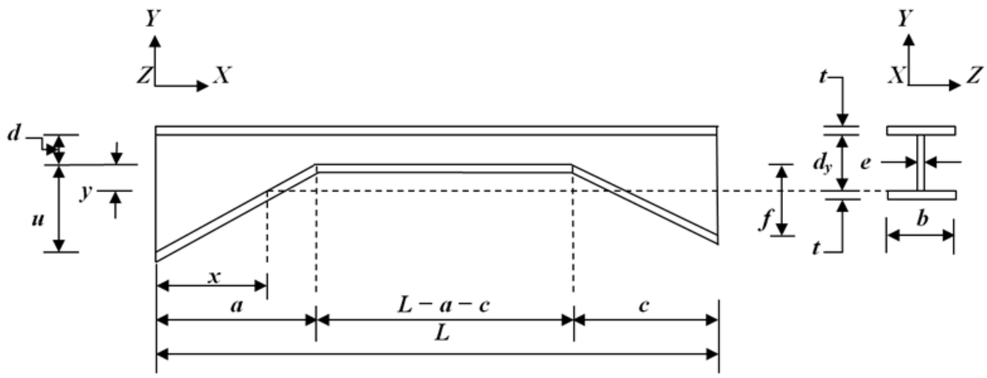


Fig. 1 I-section with straight haunches

$$A_{sx2} = e(d + 2t) \tag{5}$$

$$I_{z2} = \frac{b(d + 2t)^3 - (b - e)d^3}{12} \tag{6}$$

To $L - c \leq x \leq L$

$$d_{y3} = \frac{cd + f(x - L + c)}{c} \tag{7}$$

$$A_{sx3} = e\left[\frac{cd + f(x - L + c) + 2ct}{c}\right] \tag{8}$$

$$I_{z3} = \frac{b[cd + f(x - L + c) + 2ct]^3 - (b - e)[cd + f(x - L + c)]^3}{12c^3} \tag{9}$$

### 2.2 Fixed-end moments for concentrated load

Fig. 2(a) shows the beam "AB" subjected to a concentrated load localized anywhere on beam and its fixed ends. The fixed-end moments are found by the sum of the effects. The moments are considered positive in counter-clockwise, and negative in clockwise. Fig. 2(b) presents the same simply supported beam at their ends under the load applied to find the rotations "$\Theta_{Ai}$" and "$\Theta_{Bi}$", where "$i$" takes the values of 1, 2 and 3. The rotations "$\Theta_{A1}$" and "$\Theta_{B1}$" are when the concentrated load is placed on $0 \leq x \leq a$. The rotations "$\Theta_{A2}$" and "$\Theta_{B2}$" are when the concentrated load is located in $a \leq x \leq L - c$. The rotations "$\Theta_{A3}$" and "$\Theta_{B3}$" are when the concentrated load is found of $L - c \leq x \leq L$. Now, the rotations "$f_{11}$" and "$f_{21}$" are caused by the unitary moment applied in the support "A", according to Fig. 2(c), and in terms of "$f_{12}$" and "$f_{22}$" are caused by the unitary moment applied in the support "B", seen in Fig. 2(d) (Luévanos-Rojas 2012, 2013a, b).

The compatibility equations and equilibrium of the beam are (Luévanos-Rojas 2012, 2013a, b, Ghali *et al*. 2003, González Cuevas 2007, McCormac 2007)

To $0 \leq x \leq a$

$$-f_{11}M_{AB} + f_{12}M_{BA} = \Theta_{A1} \tag{10}$$

$$-f_{21}M_{AB} + f_{22}M_{BA} = \Theta_{B1} \tag{11}$$

To $a \leq x \leq L - c$

$$-f_{11}M_{AB} + f_{12}M_{BA} = \Theta_{A2} \tag{12}$$

$$-f_{21}M_{AB} + f_{22}M_{BA} = \Theta_{B2} \tag{13}$$

To $L - c \leq x \leq L$

$$-f_{11}M_{AB} + f_{12}M_{BA} = \Theta_{A3} \tag{14}$$

$$-f_{21}M_{AB} + f_{22}M_{BA} = \Theta_{B3} \tag{15}$$

Beam Fig. 2(b) is analyzed to find "$\Theta_{Ai}$" and "$\Theta_{Bi}$", the virtual work principle and taking into account the bending deformations and shear used to obtain the rotations.

Now, the values of "$\Theta_{Ai}$" and "$\Theta_{Bi}$" for non-prismatic members are found by the following equations

$$\Theta_{Ai} = \int_0^L \frac{V_x V_1}{GA_{sx}(x)}dx + \int_0^L \frac{M_x M_1}{EI_z(x)}dx \tag{16}$$

$$\Theta_{Bi} = \int_0^L \frac{V_x V_2}{GA_{sx}(x)}dx + \int_0^L \frac{M_x M_2}{EI_z(x)}dx \tag{17}$$

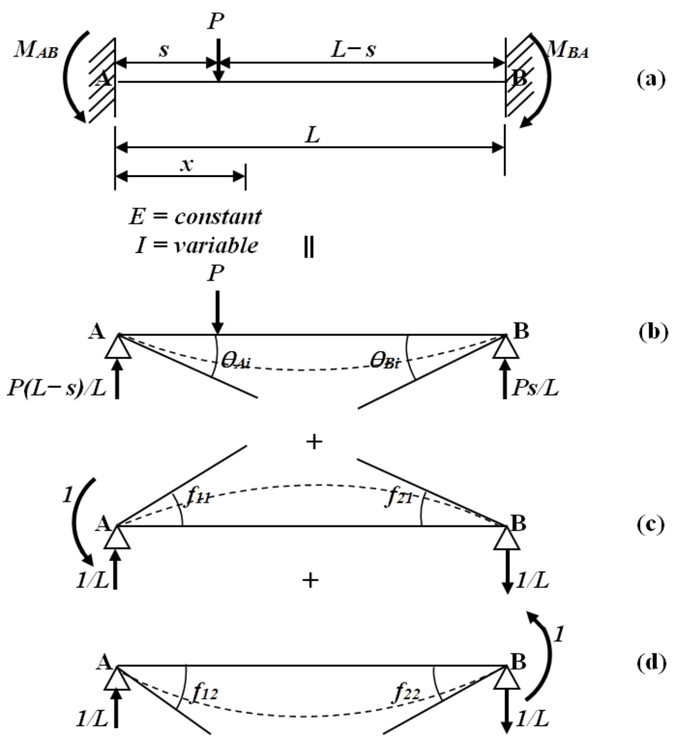


Fig. 2 Beam fixed at its ends

where: $E$ is the modulus of elasticity, $G$ is shear modulus, $V_x$ and $M_x$ is shear force and the bending moment of the real concentrated load, $V_1$ and $M_1$ is shear force and the bending moment due the unitary moment applied in the support "$A$", $V_2$ and $M_2$ is shear force and the bending moment due the unitary moment applied in the support "$B$" to a distance "$x$".

The shear modulus is

$$G = \frac{E}{2(1+\nu)} \tag{18}$$

where $\nu$ is Poisson's ratio.

Table 1 presents the equations of the shear forces and bending moments anywhere of the beam on the axis "$x$" (Gere and Goodno 2009).

Using Eqs. (16)-(17) to obtain the values of "$\Theta_{A1}$", "$\Theta_{B1}$", "$\Theta_{A2}$", "$\Theta_{B2}$", "$\Theta_{A3}$" and "$\Theta_{B3}$"

$$\begin{aligned}\Theta_{A1} = \frac{2P}{EL^2}\Bigg\{&(L-s)\int_0^s\left[\frac{1+\nu}{A_{sx1}}-\frac{(L-x)x}{2I_{z1}}\right]dx \\ &-s\int_s^a\left[\frac{1+\nu}{A_{sx1}}+\frac{(L-x)^2}{2I_{z1}}\right]dx \\ &-s\int_a^{L-c}\left[\frac{1+\nu}{A_{sx2}}+\frac{(L-x)^2}{2I_{z2}}\right]dx \\ &-s\int_{L-c}^{L}\left[\frac{1+\nu}{A_{sx3}}+\frac{(L-x)^2}{2I_{z3}}\right]dx\Bigg\}\end{aligned} \tag{19}$$

$$\begin{aligned}\Theta_{B1} = \frac{2P}{EL^2}\Bigg\{&(L-s)\int_0^s\left[\frac{1+\nu}{A_{sx1}}+\frac{x^2}{2I_{z1}}\right]dx \\ &-s\int_s^a\left[\frac{1+\nu}{A_{sx1}}-\frac{(L-x)x}{2I_{z1}}\right]dx \\ &-s\int_{L-c}^{L}\left[\frac{1+\nu}{A_{sx3}}-\frac{(L-x)x}{2I_{z3}}\right]dx\Bigg\}\end{aligned} \tag{20}$$

$$\begin{aligned}\Theta_{A2} = \frac{2P}{EL^2}\Bigg\{&(L-s)\int_0^a\left[\frac{1+\nu}{A_{sx1}}-\frac{(L-x)x}{2I_{z1}}\right]dx \\ &+(L-s)\int_a^s\left[\frac{1+\nu}{A_{sx2}}-\frac{(L-x)x}{2I_{z2}}\right]dx \\ &-s\int_s^{L-c}\left[\frac{1+\nu}{A_{sx2}}+\frac{(L-x)^2}{2I_{z2}}\right]dx \\ &-s\int_{L-c}^{L}\left[\frac{1+\nu}{A_{sx3}}+\frac{(L-x)^2}{2I_{z3}}\right]dx\Bigg\}\end{aligned} \tag{21}$$

Table 1 Shear force and the bending moment

| Concept | | Equations | | |
|---|---|---|---|---|
| Shear force | To the left of P | $V_x = \frac{P(L-s)}{L}$ | $V_1 = \frac{1}{L}$ | $V_2 = \frac{1}{L}$ |
| | To the right of P | $V_x = -\frac{Ps}{L}$ | | |
| Bending moment | To the left of P | $M_x = \frac{P(L-s)x}{L}$ | $M_1 = -\frac{(L-x)}{L}$ | $M_2 = \frac{x}{L}$ |
| | To the right of P | $M_x = \frac{Ps(L-x)}{L}$ | | |

$$\begin{aligned}\Theta_{B2} = \frac{2P}{EL^2}\Bigg\{&(L-s)\int_0^a\left[\frac{1+\nu}{A_{sx1}}+\frac{x^2}{2I_{z1}}\right]dx \\ &+(L-s)\int_a^s\left[\frac{1+\nu}{A_{sx2}}+\frac{x^2}{2I_{z2}}\right]dx \\ &-s\int_s^{L-c}\left[\frac{1+\nu}{A_{sx2}}-\frac{(L-x)x}{2I_{z2}}\right]dx \\ &-s\int_{L-c}^{L}\left[\frac{1+\nu}{A_{sx3}}-\frac{(L-x)x}{2I_{z3}}\right]dx\Bigg\}\end{aligned} \tag{22}$$

$$\begin{aligned}\Theta_{A3} = \frac{2P}{EL^2}\Bigg\{&(L-s)\int_0^a\left[\frac{1+\nu}{A_{sx1}}-\frac{(L-x)x}{2I_{z1}}\right]dx \\ &+(L-s)\int_a^{L-c}\left[\frac{1+\nu}{A_{sx2}}-\frac{(L-x)x}{2I_{z2}}\right]dx \\ &+(L-s)\int_{L-c}^{s}\left[\frac{1+\nu}{A_{sx3}}-\frac{(L-x)x}{2I_{z3}}\right]dx \\ &-s\int_s^{L}\left[\frac{1+\nu}{A_{sx3}}+\frac{(L-x)^2}{2I_{z3}}\right]dx\Bigg\}\end{aligned} \tag{23}$$

$$\begin{aligned}\Theta_{B3} = \frac{2P}{EL^2}\Bigg\{&(L-s)\int_0^a\left[\frac{1+\nu}{A_{sx1}}+\frac{x^2}{2I_{z1}}\right]dx \\ &+(L-s)\int_a^{L-c}\left[\frac{1+\nu}{A_{sx2}}+\frac{x^2}{2I_{z2}}\right]dx \\ &+(L-s)\int_{L-c}^{s}\left[\frac{1+\nu}{A_{sx3}}+\frac{x^2}{2I_{z3}}\right]dx \\ &-s\int_s^{L}\left[\frac{1+\nu}{A_{sx3}}-\frac{(L-x)x}{2I_{z3}}\right]dx\Bigg\}\end{aligned} \tag{24}$$

The coefficients of flexibilities through the virtual work principle are obtained

$$f_{11} = \int_0^L \frac{V_1V_1}{GA_{sx}(x)}dx + \int_0^L \frac{M_1M_1}{EI_z(x)}dx \tag{25}$$

$$f_{22} = \int_0^L \frac{V_2V_2}{GA_{sx}(x)}dx + \int_0^L \frac{M_2M_2}{EI_z(x)}dx \tag{26}$$

$$f_{12} = f_{21} = \int_0^L \frac{V_1V_2}{GA_{sx}(x)}dx + \int_0^L \frac{M_1M_2}{EI_z(x)}dx \tag{27}$$

Eqs. (25)-(26)-(27) are used to obtain the values of "$f_{11}$", "$f_{22}$" y "$f_{12}$" (Luévanos-Rojas 2015)

$$\begin{aligned}f_{11} = \frac{2}{EL^2}\Bigg\{&\int_0^a\left[\frac{1+\nu}{A_{sx1}}+\frac{(L-x)^2}{2I_{z1}}\right]dx \\ &+\int_a^{L-c}\left[\frac{1+\nu}{A_{sx2}}+\frac{(L-x)^2}{2I_{z2}}\right]dx \\ &+\int_{L-c}^{L}\left[\frac{1+\nu}{A_{sx3}}+\frac{(L-x)^2}{2I_{z3}}\right]dx\Bigg\}\end{aligned} \tag{28}$$

$$f_{22} = \frac{2}{EL^2}\left\{\int_0^a \left[\frac{1+\nu}{A_{sx1}} + \frac{x^2}{2I_{z1}}\right]dx + \int_a^{L-c} \left[\frac{1+\nu}{A_{sx2}} + \frac{x^2}{2I_{z2}}\right]dx + \int_{L-c}^{L} \left[\frac{1+\nu}{A_{sx3}} + \frac{x^2}{2I_{z3}}\right]dx\right\} \quad (29)$$

$$f_{12} = f_{21} = \frac{2}{EL^2}\left\{\int_0^a \left[\frac{1+\nu}{A_{sx1}} - \frac{(L-x)x}{2I_{z1}}\right]dx + \int_a^{L-c} \left[\frac{1+\nu}{A_{sx2}} - \frac{(L-x)x}{2I_{z2}}\right]dx + \int_{L-c}^{L} \left[\frac{1+\nu}{A_{sx3}} - \frac{(L-x)x}{2I_{z3}}\right]dx\right\} \quad (30)$$

First condition: The concentrated load "P" is found $0 \le x \le a$. Eqs. (19)-(28)-(30) corresponding to the support "A" are substituted into Eq. (10), and Eqs. (20)-(29)-(30) corresponding to the support "B" are substituted into Eq. (11). Subsequently, the generated equations are solved to obtain the values of "$M_{AB}$" and "$M_{BA}$"; these are shown in Eqs. (31)-(32).

Second condition: The concentrated load "$P$" is localized $a \le x \le L - c$. Eqs. (21)-(28)-(30) corresponding to the support "A" are substituted into Eq. (10), and Eqs. (22)-(29)-(30) corresponding to the support "B" are substituted into Eq. (11). Subsequently, the generated equations are solved to find the values of "$M_{AB}$" and "$M_{BA}$"; these are presented in Eqs. (33)-(34).

Third condition: The concentrated load "$P$" is placed $L - c \le x \le L$. Eqs. (23)-(28)-(30) corresponding to the support "A" are substituted into Eq. (10), and Eqs. (24)-(29)-(30) corresponding to the support "$B$" are substituted into Eq. (11). Subsequently, the generated equations are solved to obtain the values of "$M_{AB}$" and "$M_{BA}$"; these appear in Eqs. (35)-(36).

Eqs. (31)-(32)-(33)-(34)-(35)-(36) are shown in the appendix.

## 3. Validating the proposed model

Tables 2-3 show the results of the two models for the fixed-end moments factors ($m_{AB}$ and $m_{BA}$) for a beam subjected to a concentrated load located anywhere on the beam. The proposed model (*PM*) is the mathematical model presented in this paper, the bending deformations and shear are considered, and the traditional model (*TM*) takes into account only the bending deformations. Table 2 for $L = 20\ d \rightarrow d = 0.05\ L$. Table 3 for $L = 10\ d \rightarrow d = 0.10\ L$. These comparisons were made for $\nu = 0.30$ (structural steel), $b = 13.02\ t \rightarrow t = 0.0768\ b$, $d = 26.91\ e \rightarrow e = 0.0372\ d$, $b = 0.813\ d$, $u = f$, because these values are presented in Tables Appendix B (Tena-Colunga 2007). The results appearing in Table 2 (proposed model) mentioned above are identical to the Tables shown in Appendix B (Tena-Colunga 2007).

Other way to validate the proposed model is as follows: To the first condition is substituted "$u = 0\ h$ and $f = 0\ h$" or "$a = L$, $c = 0\ L$ and $u = 0\ h$" into Eqs. (31)-(32). To the second condition is substituted "$a = 0\ L$ and $c = 0\ L$" or "$u = 0h$ and $f = 0h$" into Eqs. (33)-(34). To the third condition is substituted "$u = 0\ h$ and $f = 0\ h$" or "$a = 0\ L$, $c = L$ and $f = 0h$" into Eqs. (35)-(36). To all the conditions are neglected the shear deformations. The results obtained for the three conditions, the fixed-end moments are: "$M_{AB} = Ps(L-s)^2/L^2$" and "$M_{BA} = Ps^2(L-s)/L^2$". The values presented above are for a constant cross section.

A way to validate the continuity of the cross section is as follows: when the slope of the beam in the lower face varies, i.e., when the positive slope changes to the horizontal slopffae of the straight line in "$a$", and the horizontal slope changes to the negative slope in "$L - c$", the concentrated load is placed on these points, and the fixed-end moments are the same results. For example, substituting "$s = a$" into Eqs. (31)-(33) to obtain "$M_{AB}$" and also into Eqs. (32)-(34) to found "$M_{BA}$", and now substituting "$s = L - c$" into Eqs. (33)-(35) to found "$M_{AB}$" and also into Eqs. (34)-(36) to obtain "$M_{BA}$".

Then the model proposed in this paper is valid and is not limited to certain dimensions or proportions as some authors show, and also the bending and shear deformations are considered.

## 4. Application

A continuous road bridge of three stretches for a beam of variable I-section with straight haunches is illustrated in Fig. 3. The first and third light (A-B and C-D) are of 12.00 m, and contains antisymmetric haunches and deferential depths in its ends. The second light (B-C) is 15.00 m, but the haunches are perfectly symmetrical. Fig. 4 shows the

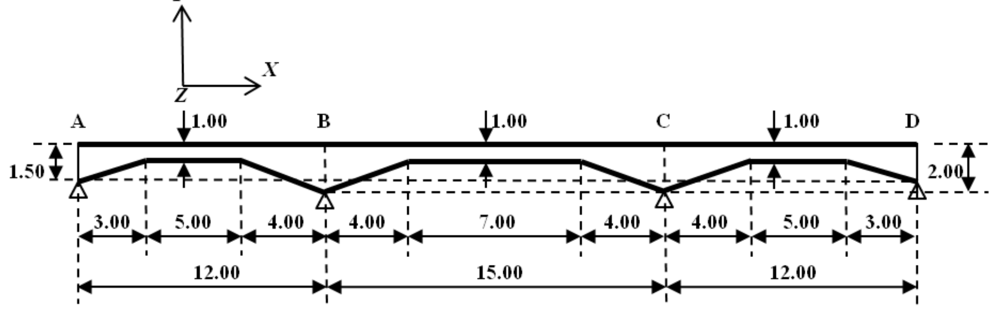


Fig. 3 Highway bridge of structural steel beams with straight haunches

Table 2 Fixed-end moments for $d$ = 0.05 L

| | | $M_{AB} = m_{AB}PL$; $M_{BA} = m_{BA}PL$ | | | | | | | | | | | | | | | | | | | |
|---|---|---|---|---|---|---|---|---|---|---|---|---|---|---|---|---|---|---|---|---|---|
| | | $s$ = 0.1 L | | | | $s$ = 0.3 L | | | | $s$ = 0.5 L | | | | $s$ = 0.7 L | | | | $s$ = 0.9 L | | | |
| $c$ | $f/d$ | $m_{AB}$ | | $m_{BA}$ | | $m_{AB}$ | | $m_{BA}$ | | $m_{AB}$ | | $m_{BA}$ | | $m_{AB}$ | | $m_{BA}$ | | $m_{AB}$ | | $m_{BA}$ | |
| | | *MP* | *MT* | *MP* | *MT* | *MP* | *MT* | *MP* | *MT* | *MP* | *MT* | *MP* | *MT* | *MP* | *MT* | *MP* | *MT* | *MP* | *MT* | *MP* | *MT* |
| $a$ = 0.1 L | | | | | | | | | | | | | | | | | | | | | |
| 0.1 L | 0.5 | 0.0852 | 0.0873 | 0.0087 | 0.0065 | 0.1575 | 0.1605 | 0.0650 | 0.0620 | 0.1327 | 0.1327 | 0.1327 | 0.1327 | 0.0650 | 0.0620 | 0.1575 | 0.1605 | 0.0087 | 0.0065 | 0.0852 | 0.0873 |
| | 1.0 | 0.0887 | 0.0909 | 0.0071 | 0.0049 | 0.1652 | 0.1685 | 0.0641 | 0.0608 | 0.1369 | 0.1369 | 0.1369 | 0.1369 | 0.0641 | 0.0608 | 0.1652 | 0.1685 | 0.0071 | 0.0049 | 0.0887 | 0.0909 |
| | 1.5 | 0.0910 | 0.0931 | 0.0060 | 0.0038 | 0.1702 | 0.1738 | 0.0633 | 0.0597 | 0.1395 | 0.1395 | 0.1395 | 0.1395 | 0.0633 | 0.0597 | 0.1702 | 0.1738 | 0.0060 | 0.0038 | 0.0910 | 0.0931 |
| | 2.0 | 0.0925 | 0.0946 | 0.0051 | 0.0031 | 0.1737 | 0.1776 | 0.0626 | 0.0588 | 0.1413 | 0.1413 | 0.1413 | 0.1413 | 0.0626 | 0.0588 | 0.1737 | 0.1776 | 0.0051 | 0.0031 | 0.0925 | 0.0946 |
| 0.3 L | 0.5 | 0.0845 | 0.0868 | 0.0103 | 0.0077 | 0.1530 | 0.1560 | 0.0757 | 0.0724 | 0.1245 | 0.1242 | 0.1516 | 0.1520 | 0.0578 | 0.0549 | 0.1723 | 0.1756 | 0.0085 | 0.0065 | 0.0847 | 0.0869 |
| | 1.0 | 0.0877 | 0.0901 | 0.0095 | 0.0066 | 0.1567 | 0.1601 | 0.0834 | 0.0795 | 0.1210 | 0.1202 | 0.1724 | 0.1734 | 0.0505 | 0.0469 | 0.1930 | 0.1972 | 0.0068 | 0.0049 | 0.0881 | 0.0904 |
| | 1.5 | 0.0897 | 0.0923 | 0.0088 | 0.0056 | 0.1585 | 0.1621 | 0.0895 | 0.0851 | 0.1169 | 0.1156 | 0.1890 | 0.1907 | 0.0441 | 0.0401 | 0.2089 | 0.2139 | 0.0056 | 0.0038 | 0.0904 | 0.0928 |
| | 2.0 | 0.0912 | 0.0938 | 0.0081 | 0.0048 | 0.1594 | 0.1631 | 0.0944 | 0.0896 | 0.1131 | 0.1112 | 0.2025 | 0.2049 | 0.0388 | 0.0343 | 0.2213 | 0.2271 | 0.0047 | 0.0029 | 0.0921 | 0.0944 |
| 0.5 L | 0.5 | 0.0842 | 0.0866 | 0.0112 | 0.0083 | 0.1512 | 0.1543 | 0.0799 | 0.0761 | 0.1214 | 0.1216 | 0.1549 | 0.1547 | 0.0569 | 0.0545 | 0.1678 | 0.1707 | 0.0088 | 0.0069 | 0.0830 | 0.0854 |
| | 1.0 | 0.0871 | 0.0898 | 0.0112 | 0.0076 | 0.1528 | 0.1565 | 0.0935 | 0.0884 | 0.1149 | 0.1150 | 0.1816 | 0.1815 | 0.0496 | 0.0470 | 0.1853 | 0.1889 | 0.0074 | 0.0054 | 0.0855 | 0.0882 |
| | 1.5 | 0.0889 | 0.0918 | 0.0112 | 0.0069 | 0.1523 | 0.1563 | 0.1063 | 0.1002 | 0.1077 | 0.1074 | 0.2057 | 0.2061 | 0.0435 | 0.0407 | 0.1993 | 0.2035 | 0.0064 | 0.0045 | 0.0873 | 0.0902 |
| | 2.0 | 0.0902 | 0.0932 | 0.0112 | 0.0064 | 0.1508 | 0.1550 | 0.1182 | 0.1115 | 0.1005 | 0.0998 | 0.2276 | 0.2287 | 0.0384 | 0.0355 | 0.2108 | 0.2155 | 0.0056 | 0.0037 | 0.0887 | 0.0917 |
| $a$ = 0.3 L | | | | | | | | | | | | | | | | | | | | | |
| 0.1 L | 0.5 | 0.0847 | 0.0869 | 0.0085 | 0.0065 | 0.1723 | 0.1756 | 0.0578 | 0.0549 | 0.1516 | 0.1520 | 0.1245 | 0.1242 | 0.0757 | 0.0724 | 0.1530 | 0.1560 | 0.0103 | 0.0077 | 0.0845 | 0.0868 |
| | 1.0 | 0.0881 | 0.0904 | 0.0068 | 0.0049 | 0.1930 | 0.1972 | 0.0505 | 0.0469 | 0.1724 | 0.1734 | 0.1210 | 0.1202 | 0.0834 | 0.0795 | 0.1567 | 0.1601 | 0.0095 | 0.0066 | 0.0877 | 0.0901 |
| | 1.5 | 0.0904 | 0.0928 | 0.0056 | 0.0038 | 0.2089 | 0.2139 | 0.0441 | 0.0401 | 0.1890 | 0.1907 | 0.1169 | 0.1156 | 0.0895 | 0.0851 | 0.1585 | 0.1621 | 0.0088 | 0.0056 | 0.0897 | 0.0923 |
| | 2.0 | 0.0921 | 0.0944 | 0.0047 | 0.0029 | 0.2213 | 0.2271 | 0.0388 | 0.0343 | 0.2025 | 0.2049 | 0.1131 | 0.1112 | 0.0944 | 0.0896 | 0.1594 | 0.1631 | 0.0081 | 0.0048 | 0.0912 | 0.0938 |
| 0.3 L | 0.5 | 0.0839 | 0.0863 | 0.0101 | 0.0078 | 0.1677 | 0.1710 | 0.0677 | 0.0644 | 0.1427 | 0.1427 | 0.1427 | 0.1427 | 0.0677 | 0.0644 | 0.1677 | 0.1710 | 0.0101 | 0.0078 | 0.0839 | 0.0863 |
| | 1.0 | 0.0869 | 0.0895 | 0.0092 | 0.0066 | 0.1844 | 0.1886 | 0.0667 | 0.0625 | 0.1542 | 0.1542 | 0.1542 | 0.1542 | 0.0667 | 0.0625 | 0.1844 | 0.1886 | 0.0092 | 0.0066 | 0.0869 | 0.0895 |
| | 1.5 | 0.0888 | 0.0916 | 0.0084 | 0.0057 | 0.1972 | 0.2024 | 0.0643 | 0.0592 | 0.1623 | 0.1623 | 0.1623 | 0.1623 | 0.0643 | 0.0592 | 0.1972 | 0.2024 | 0.0084 | 0.0057 | 0.0888 | 0.0916 |
| | 2.0 | 0.0903 | 0.0931 | 0.0077 | 0.0049 | 0.2076 | 0.2136 | 0.0614 | 0.0553 | 0.1681 | 0.1681 | 0.1681 | 0.1681 | 0.0614 | 0.0553 | 0.2076 | 0.2136 | 0.0077 | 0.0049 | 0.0903 | 0.0931 |
| 0.5 L | 0.5 | 0.0836 | 0.0861 | 0.0109 | 0.0083 | 0.1658 | 0.1693 | 0.0715 | 0.0677 | 0.1392 | 0.1398 | 0.1459 | 0.1453 | 0.0664 | 0.0637 | 0.1631 | 0.1660 | 0.0104 | 0.0081 | 0.0822 | 0.0847 |
| | 1.0 | 0.0862 | 0.0890 | 0.0108 | 0.0076 | 0.1803 | 0.1850 | 0.0751 | 0.0698 | 0.1468 | 0.1480 | 0.1627 | 0.1614 | 0.0652 | 0.0622 | 0.1763 | 0.1797 | 0.0099 | 0.0073 | 0.0841 | 0.0870 |
| | 1.5 | 0.0879 | 0.0910 | 0.0107 | 0.0070 | 0.1910 | 0.1968 | 0.0774 | 0.0705 | 0.1506 | 0.1524 | 0.1772 | 0.1751 | 0.0631 | 0.0599 | 0.1866 | 0.1904 | 0.0095 | 0.0067 | 0.0853 | 0.0887 |
| | 2.0 | 0.0890 | 0.0924 | 0.0105 | 0.0064 | 0.1992 | 0.2061 | 0.0787 | 0.0703 | 0.1520 | 0.1543 | 0.1901 | 0.1874 | 0.0606 | 0.0572 | 0.1950 | 0.1992 | 0.0091 | 0.0061 | 0.0862 | 0.0899 |

Table 3 Fixed-end moments for $d$ = 0.10 L

| | | $M_{AB} = m_{AB}PL$; $M_{BA} = m_{BA}PL$ | | | | | | | | | | | | | | | | | | | |
|---|---|---|---|---|---|---|---|---|---|---|---|---|---|---|---|---|---|---|---|---|---|
| | | $s$ = 0.1 L | | | | $s$ = 0.3 L | | | | $s$ = 0.5 L | | | | $s$ = 0.7 L | | | | $s$ = 0.9 L | | | |
| $c$ | $f/d$ | $m_{AB}$ | | $m_{BA}$ | | $m_{AB}$ | | $m_{BA}$ | | $m_{AB}$ | | $m_{BA}$ | | $m_{AB}$ | | $m_{BA}$ | | $m_{AB}$ | | $m_{BA}$ | |
| | | *PM* | *TM* | *PM* | *TM* | *PM* | *TM* | *PM* | *TM* | *PM* | *TM* | *PM* | *TM* | *PM* | *TM* | *PM* | *TM* | *PM* | *TM* | *PM* | *TM* |
| | | $a$ = 0.1 L | | | | | | | | | | | | | | | | | | | |
| 0.1 L | 0.5 | 0.0801 | 0.0873 | 0.0138 | 0.0065 | 0.1506 | 0.1605 | 0.0719 | 0.0620 | 0.1327 | 0.1327 | 0.1327 | 0.1327 | 0.0719 | 0.0620 | 0.1506 | 0.1605 | 0.0138 | 0.0065 | 0.0801 | 0.0873 |
| | 1.0 | 0.0837 | 0.0909 | 0.0121 | 0.0049 | 0.1574 | 0.1685 | 0.0719 | 0.0608 | 0.1369 | 0.1369 | 0.1369 | 0.1369 | 0.0719 | 0.0608 | 0.1574 | 0.1685 | 0.0121 | 0.0049 | 0.0837 | 0.0909 |
| | 1.5 | 0.0861 | 0.0931 | 0.0108 | 0.0038 | 0.1619 | 0.1738 | 0.0716 | 0.0597 | 0.1395 | 0.1395 | 0.1395 | 0.1395 | 0.0716 | 0.0597 | 0.1619 | 0.1738 | 0.0108 | 0.0038 | 0.0861 | 0.0931 |
| | 2.0 | 0.0878 | 0.0946 | 0.0098 | 0.0031 | 0.1651 | 0.1776 | 0.0712 | 0.0588 | 0.1413 | 0.1413 | 0.1413 | 0.1413 | 0.0712 | 0.0588 | 0.1651 | 0.1776 | 0.0098 | 0.0031 | 0.0878 | 0.0946 |
| 0.3 L | 0.5 | 0.0792 | 0.0868 | 0.0162 | 0.0077 | 0.1462 | 0.1560 | 0.0832 | 0.0724 | 0.1252 | 0.1242 | 0.1508 | 0.1520 | 0.0646 | 0.0549 | 0.1648 | 0.1756 | 0.0131 | 0.0065 | 0.0796 | 0.0869 |
| | 1.0 | 0.0823 | 0.0901 | 0.0159 | 0.0066 | 0.1494 | 0.1601 | 0.0922 | 0.0795 | 0.1228 | 0.1202 | 0.1703 | 0.1734 | 0.0582 | 0.0469 | 0.1837 | 0.1972 | 0.0111 | 0.0049 | 0.0831 | 0.0904 |
| | 1.5 | 0.0843 | 0.0923 | 0.0155 | 0.0056 | 0.1509 | 0.1621 | 0.0989 | 0.0851 | 0.1198 | 0.1156 | 0.1855 | 0.1907 | 0.0527 | 0.0401 | 0.1982 | 0.2139 | 0.0096 | 0.0038 | 0.0855 | 0.0928 |
| | 2.0 | 0.0858 | 0.0938 | 0.0150 | 0.0048 | 0.1517 | 0.1631 | 0.1042 | 0.0896 | 0.1170 | 0.1112 | 0.1975 | 0.2049 | 0.0480 | 0.0343 | 0.2095 | 0.2271 | 0.0084 | 0.0029 | 0.0873 | 0.0944 |
| 0.5 L | 0.5 | 0.0788 | 0.0866 | 0.0177 | 0.0083 | 0.1440 | 0.1543 | 0.0886 | 0.0761 | 0.1210 | 0.1216 | 0.1554 | 0.1547 | 0.0625 | 0.0545 | 0.1610 | 0.1707 | 0.0133 | 0.0069 | 0.0776 | 0.0854 |
| | 1.0 | 0.0814 | 0.0898 | 0.0190 | 0.0076 | 0.1449 | 0.1565 | 0.1043 | 0.0884 | 0.1147 | 0.1150 | 0.1819 | 0.1815 | 0.0551 | 0.0470 | 0.1777 | 0.1889 | 0.0115 | 0.0054 | 0.0799 | 0.0882 |
| | 1.5 | 0.0832 | 0.0918 | 0.0199 | 0.0069 | 0.1441 | 0.1563 | 0.1185 | 0.1002 | 0.1081 | 0.1074 | 0.2051 | 0.2061 | 0.0491 | 0.0407 | 0.1909 | 0.2035 | 0.0102 | 0.0045 | 0.0816 | 0.0902 |
| | 2.0 | 0.0844 | 0.0932 | 0.0205 | 0.0064 | 0.1427 | 0.1550 | 0.1311 | 0.1115 | 0.1018 | 0.0998 | 0.2254 | 0.2287 | 0.0441 | 0.0355 | 0.2016 | 0.2155 | 0.0092 | 0.0037 | 0.0829 | 0.0917 |
| | | $a$ = 0.3 L | | | | | | | | | | | | | | | | | | | |
| 0.1 L | 0.5 | 0.0796 | 0.0869 | 0.0131 | 0.0065 | 0.1648 | 0.1756 | 0.0646 | 0.0549 | 0.1508 | 0.1520 | 0.1252 | 0.1242 | 0.0832 | 0.0724 | 0.1462 | 0.1560 | 0.0162 | 0.0077 | 0.0792 | 0.0868 |
| | 1.0 | 0.0831 | 0.0904 | 0.0111 | 0.0049 | 0.1837 | 0.1972 | 0.0582 | 0.0469 | 0.1703 | 0.1734 | 0.1228 | 0.1202 | 0.0922 | 0.0795 | 0.1494 | 0.1601 | 0.0159 | 0.0066 | 0.0823 | 0.0901 |
| | 1.5 | 0.0855 | 0.0928 | 0.0096 | 0.0038 | 0.1982 | 0.2139 | 0.0527 | 0.0401 | 0.1855 | 0.1907 | 0.1198 | 0.1156 | 0.0989 | 0.0851 | 0.1509 | 0.1621 | 0.0155 | 0.0056 | 0.0843 | 0.0923 |
| | 2.0 | 0.0873 | 0.0944 | 0.0084 | 0.0029 | 0.2095 | 0.2271 | 0.0480 | 0.0343 | 0.1975 | 0.2049 | 0.1170 | 0.1112 | 0.1042 | 0.0896 | 0.1517 | 0.1631 | 0.0150 | 0.0048 | 0.0858 | 0.0938 |
| 0.3 L | 0.5 | 0.0786 | 0.0863 | 0.0154 | 0.0078 | 0.1603 | 0.1710 | 0.0750 | 0.0644 | 0.1427 | 0.1427 | 0.1427 | 0.1427 | 0.0750 | 0.0644 | 0.1603 | 0.1710 | 0.0154 | 0.0078 | 0.0786 | 0.0863 |
| | 1.0 | 0.0814 | 0.0895 | 0.0147 | 0.0066 | 0.1755 | 0.1886 | 0.0755 | 0.0625 | 0.1542 | 0.1542 | 0.1542 | 0.1542 | 0.0755 | 0.0625 | 0.1755 | 0.1886 | 0.0147 | 0.0066 | 0.0814 | 0.0895 |
| | 1.5 | 0.0834 | 0.0916 | 0.0139 | 0.0057 | 0.1871 | 0.2024 | 0.0745 | 0.0592 | 0.1623 | 0.1623 | 0.1623 | 0.1623 | 0.0745 | 0.0592 | 0.1871 | 0.2024 | 0.0139 | 0.0057 | 0.0834 | 0.0916 |
| | 2.0 | 0.0849 | 0.0931 | 0.0131 | 0.0049 | 0.1963 | 0.2136 | 0.0726 | 0.0553 | 0.1681 | 0.1681 | 0.1681 | 0.1681 | 0.0726 | 0.0553 | 0.1963 | 0.2136 | 0.0131 | 0.0049 | 0.0849 | 0.0931 |
| 0.5 L | 0.5 | 0.0782 | 0.0861 | 0.0168 | 0.0083 | 0.1580 | 0.1693 | 0.0799 | 0.0677 | 0.1379 | 0.1398 | 0.1473 | 0.1453 | 0.0724 | 0.0637 | 0.1566 | 0.1660 | 0.0156 | 0.0081 | 0.0766 | 0.0847 |
| | 1.0 | 0.0805 | 0.0890 | 0.0173 | 0.0076 | 0.1708 | 0.1850 | 0.0859 | 0.0698 | 0.1444 | 0.1480 | 0.1654 | 0.1614 | 0.0712 | 0.0622 | 0.1695 | 0.1797 | 0.0152 | 0.0073 | 0.0781 | 0.0870 |
| | 1.5 | 0.0821 | 0.0910 | 0.0175 | 0.0070 | 0.1802 | 0.1968 | 0.0901 | 0.0705 | 0.1474 | 0.1524 | 0.1810 | 0.1751 | 0.0691 | 0.0599 | 0.1795 | 0.1904 | 0.0147 | 0.0067 | 0.0791 | 0.0887 |
| | 2.0 | 0.0833 | 0.0924 | 0.0176 | 0.0064 | 0.1874 | 0.2061 | 0.0931 | 0.0703 | 0.1482 | 0.1543 | 0.1947 | 0.1874 | 0.0665 | 0.0572 | 0.1878 | 0.1992 | 0.0142 | 0.0061 | 0.0800 | 0.0899 |

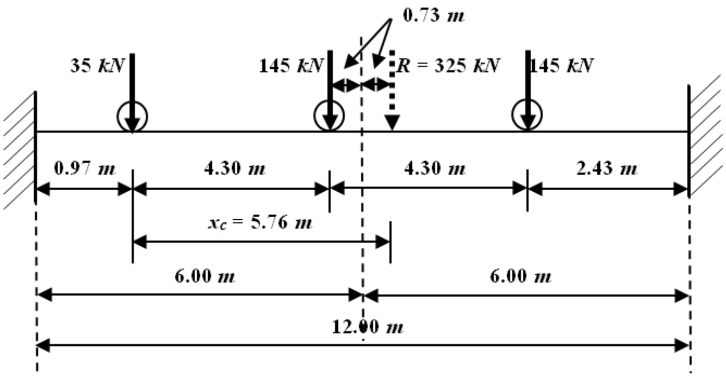


(a) To first and third light (A-B and C-D)

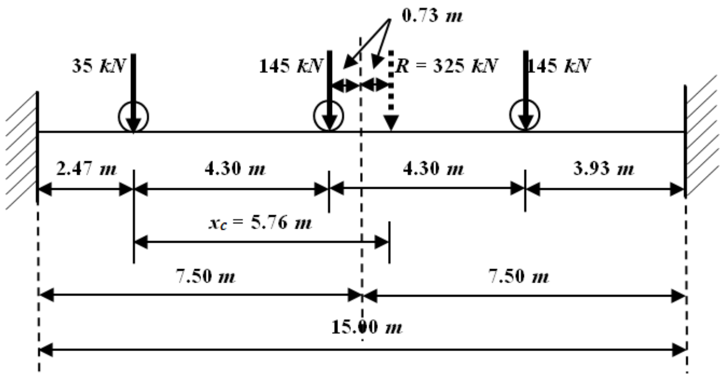


(b) To second light (B-C)

Fig. 4 Critical position of the loads

critical position of the live loads for each stretch of the highway bridge and taking into account the live loads that provide specifications for the design of bridges (AASHTO 2014). Constant data over all the cross section are: $b$ = 0.75 $m$, $t$ = 0.05 $m$, $e$ = 0.032 $m$. To obtain the final moments using the proposed model by means of matrix methods.

For the beam A-B: $a$ = 3.00 $m$; $c$ = 4.00 $m$; $d$ = 0.90 $m$; $u$ = 0.50 $m$; $f$ = 1.00 $m$; $L$ = 12.00 $m$. To the load $P$ = 35 $kN$, $s$ = 0.97 $m$, and is localized of $0 \leq x \leq a$, the fixed-end moments are: $M_{AB1}$ = 28.3928 $kN$-$m$ and $M_{BA1}$ = 4.7250 $kN$-$m$. To the load $P$ = 145 $kN$, $s$ = 5.27 $m$, and is found of $a \leq x \leq L - c$, the fixed-end moments are: $M_{AB2}$ = 249.7065 $kN$-$m$ and $M_{BA2}$ = 267.1544 kN-m. To the load $P$ = 145 $kN$, $s$ = 9.57 $m$, and is located of $L - c \leq x \leq L$, the fixed-end moments are: $M_{AB3}$ = 48.8118 $kN$-$m$ and $M_{BA3}$ = 265.9288 $kN$-$m$. The total fixed-end moments are: $M_{ABT}$ = 326.9111 $kN$-$m$ and $M_{BAT}$ = 537.8082 $kN$-$m$. The carry-over factors are (Luévanos-Rojas 2015): $C_{AB}$ = 0.6412 and $C_{BA}$ = 0.4996. The stiffness factors are (Luévanos-Rojas 2015): $k_{AB}$ = 5.5904 and $k_{BA}$ = 7.1748. The absolute stiffnesses are: $K_{AB}$ = 5.5904 $EI/L$ and $K_{BA}$ = 7.1748 $EI/L$.

For the beam B-C: $a$ = 4.00 $m$; $c$ = 4.00 $m$; $d$ = 0.90 $m$; $u$ = 1.00 $m$; $f$ = 1.00 $m$; $L$ = 15.00 $m$. To the load $P$ = 35 $kN$, $s$ = 2.47 $m$, and is localized of $0 \leq x \leq a$, the fixed-end moments are: $M_{BC1}$ = 69.5804 $kN$-$m$ and $M_{CB1}$ = 11.3585 $kN$-$m$. To the load $P$ = 145 $kN$, $s$ = 6.77 $m$, and is found of $a \leq x \leq L - c$, the fixed-end moments are: $M_{BC2}$ = 370.9744 $kN$-$m$ and $M_{CB2}$ = 292.3753 $kN$-$m$. To the load $P$ = 145 $kN$, $s$ = 11.07 $m$, and is located of $L - c \leq x \leq L$, the fixed-end moments are: $M_{BC3}$ = 111.3617 $kN$-$m$ and $M_{CB3}$ = 386.8492 $kN$-$m$. The total fixed-end moments are: $M_{BCT}$ = 551.9165 $kN$-$m$ and $M_{CBT}$ = 690.5830 $kN$-$m$. The carry-over factors are (Luévanos-Rojas 2015): $C_{BC}$ = 0.6121 and $C_{CB}$ = 0.6121. The stiffness factors are (Luévanos-Rojas 2015): $k_{BC}$ = 7.2120 and $k_{CB}$ = 7.2120. The absolute stiffnesses are: $K_{BC}$ = 7.2120 $EI/L$ and $K_{CB}$ = 7.2120 $EI/L$.

For the beam C-D: $a$ = 4.00 $m$; $c$ = 3.00 $m$; $d$ = 0.90 $m$; $u$ = 1.00 $m$; $f$ = 0.50 $m$; $L$ = 12.00 $m$. To the load $P$ = 35 $kN$, $s$ = 0.97 $m$, and is localized of $0 \leq x \leq a$, the fixed-end moments are: $M_{CD1}$ = 29.6864 $kN$-$m$ and $M_{DC1}$ = 2.8285 $kN$-$m$. To the load $P$ = 145 $kN$, $s$ = 5.27 $m$, and is found of $a \leq x \leq L - c$, the fixed-end moments are: $M_{CD2}$ = 335.0357 $kN$-$m$ and $M_{DC2}$ = 183.8729 $kN$-$m$. To the load $P$ = 145 $kN$, $s$ = 9.57 $m$, and is located of $L - c \leq x \leq L$, the fixed-end moments are: $M_{CD3}$ = 81.6770 $kN$-$m$ and $M_{DC3}$ = 236.7392 $kN$-$m$. The total fixed-end moments are: $M_{CDT}$ = 446.3991 $kN$-$m$ and $M_{DCT}$ = 423.4406 $kN$-$m$. The carry-over factors are (Luévanos-Rojas 2015): $C_{CD}$ = 0.4996 and $C_{DC}$ = 0.6412. The stiffness factors are (Luévanos-Rojas 2015): $k_{CD}$ = 7.1748 and $k_{DC}$ = 5.5904. The absolute stiffnesses are: $K_{CD}$ = 7.1748 $EI/L$ and $K_{DC}$ = 5.5904 $EI/L$.

The stiffness matrix of the beam "$AB$" is

$$K_{AB} = \begin{bmatrix} k_{11}^{AB} & k_{12}^{AB} \\ k_{21}^{AB} & k_{22}^{AB} \end{bmatrix} = \begin{bmatrix} 5.5904 & 3.5849 \\ 3.5849 & 7.1748 \end{bmatrix} \frac{EI}{L}$$

where

$$k_{11}^{AB} = K_{AB};\ k_{22}^{AB} = K_{BA};\ k_{12}^{AB} = C_{AB}K_{AB};$$
$$k_{21}^{AB} = C_{BA}K_{BA}; k_{12}^{AB} = k_{21}^{AB}.$$

The stiffness matrix of the beam “*BC*” is

$$K_{BC} = \begin{bmatrix} k_{11}^{BC} & k_{12}^{BC} \\ k_{21}^{BC} & k_{22}^{BC} \end{bmatrix} = \begin{bmatrix} 7.2120 & 4.4142 \\ 4.4142 & 7.2120 \end{bmatrix} \frac{EI}{L}$$

where

$$k_{11}^{BC} = K_{BC};\ k_{22}^{BC} = K_{CB};\ k_{12}^{BC} = C_{BC}K_{BC};$$
$$k_{21}^{BC} = C_{CB}K_{CB}; k_{12}^{BC} = k_{21}^{BC}.$$

The stiffness matrix of the beam “*CD*” is

$$K_{CD} = \begin{bmatrix} k_{11}^{CD} & k_{12}^{CD} \\ k_{21}^{CD} & k_{22}^{CD} \end{bmatrix} = \begin{bmatrix} 7.1748 & 3.5849 \\ 3.5849 & 5.5904 \end{bmatrix} \frac{EI}{L}$$

where

$$k_{11}^{CD} = K_{CD};\ k_{22}^{CD} = K_{DC};\ k_{12}^{CD} = C_{CD}K_{CD};$$
$$k_{21}^{CD} = C_{DC}K_{DC}; k_{12}^{CD} = k_{21}^{CD}.$$

The overall stiffness matrix “$K_O$” of the continuous beam is

$$K_O = \begin{bmatrix} k_{11}^{AB} & k_{12}^{AB} & 0 & 0 \\ k_{21}^{AB} & k_{22}^{AB} + k_{11}^{BC} & k_{12}^{BC} & 0 \\ 0 & k_{21}^{BC} & k_{22}^{BC} + k_{11}^{CD} & k_{12}^{CD} \\ 0 & 0 & k_{21}^{CD} & k_{22}^{CD} \end{bmatrix}$$
$$= \begin{bmatrix} 5.5904 & 3.5849 & 0 & 0 \\ 3.5849 & 14.3868 & 4.4142 & 0 \\ 0 & 4.4142 & 14.3868 & 3.5849 \\ 0 & 0 & 3.5849 & 5.5904 \end{bmatrix} \frac{EI}{L}$$

The fixed-end moments of the beams (phase 1) are

$$\begin{bmatrix} M_{AB} \\ M_{BA} \end{bmatrix} = \begin{bmatrix} +326.9111 \\ -537.8082 \end{bmatrix}; \begin{bmatrix} M_{BC} \\ M_{CB} \end{bmatrix} = \begin{bmatrix} +551.9165 \\ -690.5830 \end{bmatrix};$$
$$\begin{bmatrix} M_{CD} \\ M_{DC} \end{bmatrix} = \begin{bmatrix} +446.3991 \\ -423.4406 \end{bmatrix}$$

The vector of effective moments acting on the continuous beam is

$$\begin{bmatrix} M_A \\ M_B \\ M_C \\ M_D \end{bmatrix} = \begin{bmatrix} -326.9111 \\ +537.8082 - 551.9165 \\ +690.5830 - 446.3991 \\ +423.4406 \end{bmatrix} = \begin{bmatrix} -326.9111 \\ -14.1083 \\ +244.1839 \\ +423.4406 \end{bmatrix}$$

The force-displacement relationship is

$$[P] = [K] = [d]$$
$$\begin{bmatrix} -326.9111 \\ -14.1083 \\ +244.1839 \\ +423.4406 \end{bmatrix} = \begin{bmatrix} 5.5904 & 3.5849 & 0 & 0 \\ 3.5849 & 14.3868 & 4.4142 & 0 \\ 0 & 4.4142 & 14.3868 & 3.5849 \\ 0 & 0 & 3.5849 & 5.5904 \end{bmatrix} \frac{EI}{L} \begin{bmatrix} \theta_A \\ \theta_B \\ \theta_C \\ \theta_D \end{bmatrix}$$

The solution of the system is

$$\begin{bmatrix} \theta_A \\ \theta_B \\ \theta_C \\ \theta_D \end{bmatrix} = \begin{bmatrix} -71.05726558 \\ +19.61768459 \\ -9.426580882 \\ +81.78912954 \end{bmatrix} \frac{L}{EI}$$

The mechanical elements associated to the analysis moments (phase 2) are

$$\begin{bmatrix} M_{AB} \\ M_{BA} \end{bmatrix} = \begin{bmatrix} k_{11}^{AB} & k_{12}^{AB} \\ k_{21}^{AB} & k_{22}^{AB} \end{bmatrix} \begin{bmatrix} \theta_A \\ \theta_B \end{bmatrix}$$
$$= \begin{bmatrix} 5.5904 & 3.5849 \\ 3.5849 & 7.1748 \end{bmatrix} \frac{EI}{L} \begin{bmatrix} -71.05726558 \\ +19.61768459 \end{bmatrix} \frac{L}{EI}$$
$$= \begin{bmatrix} -326.9111 \\ -113.9802 \end{bmatrix}$$

$$\begin{bmatrix} M_{BC} \\ M_{CB} \end{bmatrix} = \begin{bmatrix} k_{11}^{BC} & k_{12}^{BC} \\ k_{21}^{BC} & k_{22}^{BC} \end{bmatrix} \begin{bmatrix} \theta_B \\ \theta_C \end{bmatrix}$$
$$= \begin{bmatrix} 7.2120 & 4.4142 \\ 4.4142 & 7.2120 \end{bmatrix} \frac{EI}{L} \begin{bmatrix} +19.61768459 \\ -9.426580882 \end{bmatrix} \frac{L}{EI}$$
$$= \begin{bmatrix} +99.8719 \\ +18.6119 \end{bmatrix}$$

$$\begin{bmatrix} M_{CD} \\ M_{DC} \end{bmatrix} = \begin{bmatrix} k_{11}^{CD} & k_{12}^{CD} \\ k_{21}^{CD} & k_{22}^{CD} \end{bmatrix} \begin{bmatrix} \theta_C \\ \theta_D \end{bmatrix}$$
$$= \begin{bmatrix} 7.1748 & 3.5849 \\ 3.5849 & 5.5904 \end{bmatrix} \frac{EI}{L} \begin{bmatrix} -9.426580882 \\ +81.78912954 \end{bmatrix} \frac{L}{EI}$$
$$= \begin{bmatrix} +225.5720 \\ +423.4406 \end{bmatrix}$$

The moments resulting from the sum of phase 1 and 2 (final moments) are

$$\begin{bmatrix} M_{AB} \\ M_{BA} \end{bmatrix} = \begin{bmatrix} +326.9111 \\ -537.8082 \end{bmatrix} + \begin{bmatrix} -326.9111 \\ -113.9802 \end{bmatrix} = \begin{bmatrix} 0 \\ -651.7884 \end{bmatrix}$$
$$\begin{bmatrix} M_{BC} \\ M_{CB} \end{bmatrix} = \begin{bmatrix} +551.9165 \\ -690.5830 \end{bmatrix} + \begin{bmatrix} +99.8719 \\ +18.6119 \end{bmatrix} = \begin{bmatrix} +651.7884 \\ -671.9711 \end{bmatrix}$$
$$\begin{bmatrix} M_{CD} \\ M_{DC} \end{bmatrix} = \begin{bmatrix} +446.3991 \\ -423.4406 \end{bmatrix} + \begin{bmatrix} +225.5720 \\ +423.4406 \end{bmatrix} = \begin{bmatrix} +671.9711 \\ 0 \end{bmatrix}$$

## 5. Results

Just as shown in Tables 2-3, the factors in the fixed-end moments were influenced by the web depth “*d*”. As the web depth of the haunches increases in support “*B*” is seen an increase in these factors for the same support and in the support “*A*” occurs a decrease, this is for the two models. Now, according to the comparison of both models, when the web depth of the haunches is greater at one end is presented a larger factor in the fixed-end moments of this support in the traditional model and the opposite end is greater the proposed model. Also, when the concentrated load is closer to one of the supports, the difference between the two models is larger. Also when the haunches and loads are symmetrical the fixed-end moments for the two models are not affected. The biggest difference exists for “$d$ = 0.1 $L$”, “$a$ = 0.3 $L$”, $c$ = 0.5$L$, “$f/d$ = 2” and “$s$ = 0.9 $L$” in support “*A*” of 2.33 times, and for “$d$ = 0.1 $L$”, “$a$ = 0.3 $L$”, $c$ = 0.5 $L$, “$f/d$ = 2” and “$s$ = 0.1 $L$” in support “*B*” of 2.75 times, being larger the proposed model for both cases with respect to the traditional model.

## 6. Conclusions

This paper presents a mathematical model for fixed-end moments of I-sections with straight haunches for the general case (symmetrical and/or non-symmetrical) subjected to a concentrated load localized anywhere on beam taking into account the bending deformations and shear, which is the novelty of this research. The properties of the cross section of the beam vary along its axis "$x$", i.e., the flange width "$b$", the flange thickness "$t$", the web thickness "$e$" are constant and the height "$d$" varies along the beam, this variation is linear type. Traditional models only consider bending deformations and other authors present some tables considering bending and shear deformations, but are limited, for example $L$ = 20 $d \rightarrow d$ = 0.05 $L$, $v$ = 0.30 (structural steel), $b$ = 13.02 $t \rightarrow t$ = 0.0768 $b$, $d$ = 26.91 $e \rightarrow e$ = 0.0372 $d$, $b$ = 0.813 $d$, $u = f$, this relationship is presented in the appendix B (Tena-Colunga 2007).

Besides the effectiveness and accuracy of the developed model in this paper, a significant advantage is that it can be applied to any cross section of type "I" of structural steel such as the profiles "W", "M" and "HP" by adapting the profile of the central section, and its main application is for profiles consisting of three welded plates, also can be applied to reinforced concrete beams or prestressed of I-sections for the bridges of large clearings.

Now, the application of the fixed-end moments due to a concentrated load located anywhere on the beam can be in the bridges where the main live load corresponds to concentrated loads transmitted by the vehicles through their tires to the surface rolling board.

In any structure, the shear forces and bending moments are present; therefore, the bending deformations and shear appear. Then, the proposed model which considers the bending deformations and shear is more appropriate for structural analysis and is also more suited to the real conditions compared to the traditional model that takes into account only the bending deformations.

## References


AASHTO (2014), AASHTO LRFD Bridge Design Specifications; (7th Edition), American Association of State and Highway Transportation Officials, Washington, D.C., USA.

Albegmprli, H.M., Çevik, A., Gülşan, M.E. and Kurtoglu, A.E. (2015), "Reliability analysis of reinforced concrete haunched beams shear capacity based on stochastic nonlinear FE analysis", *Comput. Concrete*, *Int. J.*, **15**(2), 259-277.

Brown, C.J. (1984), "Approximate stiffness matrix for tapered beams", *J. Struct. Eng.-ASCE*, **110**(12), 3050-3055.

Cristutiu, I-M., Nunes, D.L. and Dogariu, A.I. (2012), "Experimental study on laterally restrained steel columns with variable I cross sections", *Steel Compos. Struct.*, *Int. J.*, **13**(3), 225-238.

Gere, J.M. and Goodno, B.J. (2009), *Mechanics of Materials*, Cengage Learning, New York, NY, USA.

Ghali, A., Neville, A.M. and Brown, T.G. (2003), *Structural Analysis*: *A Unified Classical and Matrix Approach*, Taylor & Francis, New York, NY, USA.

González Cuevas, O.M. (2007), *Análisis Estructural*, Limusa, México.

Guldan, R. (1956), *Estructuras aporticadas y vigas continuas*, El ateneo, Buenos Aires, Argentina.

Fiore, A., Monaco, P. and Raffaele, D. (2012), "Viscoelastic behaviour of non-homogeneous variable-section beams with post-poned restraints", *Comput. Concrete*, *Int. J.*, **9**(5), 357-374.

Hibbeler, R.C. (2006), *Structural Analysis*, Prentice-Hall, Inc., NJ, USA.

Huang, D.M., Zhu, L.D. and Chen, W. (2014), "Power spectra of wind forces on a high-rise building with section varying along height", *Wind Struct.*, *Int. J.*, **18**(3), 295-320.

Just, D.J. (1977), "Plane frameworks of tapering box and I-section", *J. Struct. Eng.-ASCE*, **103**(1), 71-86.

Luévanos-Rojas, A. (2012), "Method of Structural Analysis for Statically Indeterminate Beams", *Int. J. Innov. Comput. I.*, **8**(8), 5473-5486.

Luévanos-Rojas, A. (2013a), "Method of structural analysis for statically indeterminate rigid frames", *Int. J. Innov. Comput. I.*, **9**(5), 1951-1970.

Luévanos-Rojas, A. (2013b), "Method of structural analysis, taking into account deformations by flexure, shear and axial", *Int. J. Innov. Comput. I.*, **9**(9), 3817-3838.

Luévanos-Rojas, A. (2013c), "A mathematical model for rectangular beams of variable cross section of symmetrical parabolic shape for uniformly distributed load", *Far East J. Math. Sci.*, **80**(2), 197-230.

Luévanos-Rojas, A. (2014), "A mathematical model for fixed-end moments for two types of loads for a parabolic shaped variable rectangular cross section", *Ing. Invest.*, **34**(2), 17-22.

Luévanos-Rojas, A. (2015), "Modelado para vigas de sección transversal "I" sometidas a una carga uniformemente distribuida con cartelas rectas", *Ingeniería Mecánica Tecnología y Desarrollo*, **5**(2), 281-292.

Luévanos-Rojas, A. and Montoya-Ramírez, J. (2014), "Mathematical model for rectangular beams of variable cross section of symmetrical linear shape for uniformly distributed load", *Int. J. Innov. Comput. I.*, **10**(2), 545-564.

Luévanos-Rojas, A., Luévanos-Rojas, R., Luévanos-Soto, I., Luévanos-Vazquez, R.G. and Ramírez-Luévanos, O.A. (2014), "Mathematical model for rectangular beams of variable cross section of symmetrical linear shape for concentrated load", *Int. J. Innov. Comput. I.*, **10**(3), 851-881.

McCormac, J.C. (2007), *Structural Analysis*: *Using Classical and Matrix Methods*, John Wiley & Sons, New York, NY, USA.

Medwadowski, S.J. (1984), "Nonprismatic shear beams", *J. Struct. Eng.-ASCE*, **110**(5), 1067-1082.

Portland Cement Association (PCA) (1958), *Beam Factors and Moment Coefficients for Members of Variable Cross-section*, Handbook of Frame Constants, Chicago, IL, USA.

Saffari, H., Mohammadnejad, M. and Bagheripour, M.H. (2012), "Free vibration analysis of non-prismatic beams under variable axial forces", *Struct. Eng. Mech.*, *Int. J.*, **43**(5), 561-582.

Shooshtari, A. and Khajavi, R. (2010), "An efficient procedure to find shape functions and stiffness matrices of nonprismatic Euler-Bernoulli and Timoshenko beam elements", *Eur. J. Mech. A-Solid.*, **29**(5), 826-836.

Schreyer, H.L. (1978), "Elementary theory for linearly tapered beams", *J. Struct. Eng.-ASCE*, **104**(3), 515-527.

Tena-Colunga, A. (1996), "Stiffness formulation for nonprismatic beam elements", *J. Struct. Eng.-ASCE*, **122**(12), 1484-1489.

Tena-Colunga, A. (2007), *Análisis de estructuras con métodos matriciales*, Limusa, México.

Tena-Colunga, A. and Zaldo, A. (1994), Ductilidad de marcos con trabes acarteladas y columnas de sección variable, *Reporte FJBS/CIS-94/04*, Centro de Investigación Sísmica, AC, Fundación Javier Barrios Sierra.

Vaidyanathan, R. and Perumal, P. (2005), *Structural Analysis*, Laxmi Publications (P) LTD, New Delhi, India.

Williams, A. (2008), *Structural Analysis*, Butterworth Heinemann, New York, NY, USA.

Won, S.G., Bae, S.H., Jeong, W.B., Cho, J.R. and Bae, S.R. (2012), "Forced vibration analysis of damped beam structures with composite cross-section using Timoshenko beam element", *Struct. Eng. Mech., Int. J.*, **43**(1), 15-30.

Yuksel, S.B. (2009), "Behaviour of symmetrically haunched non-prismatic members subjected to temperature changes", *Struct. Eng. Mech., Int. J.*, **31**(3), 297-314.

Yuksel, S.B. (2012), "Assessment of non-prismatic beams having symmetrical parabolic haunches with constant haunch length ratio of 0.5", *Struct. Eng. Mech., Int. J.*, **42**(6), 849-866.

*CC*

## Appendix

Eqs. (31)-(32) present the fixed-end moments, when the concentrated load "$P$" is localized $0 \le x \le a$

$$
\begin{aligned}
M_{AB} = P\Bigg[\Bigg\{&(L-s)\int_0^s \left[\frac{1+\nu}{A_{sx1}} - \frac{(L-x)x}{2I_{z1}}\right]dx \\
&-s\int_s^a \left[\frac{1+\nu}{A_{sx1}} + \frac{(L-x)^2}{2I_{z1}}\right]dx \\
&-s\int_a^{L-c} \left[\frac{1+\nu}{A_{sx2}} + \frac{(L-x)^2}{2I_{z2}}\right]dx \\
&-s\int_{L-c}^L \left[\frac{1+\nu}{A_{sx3}} + \frac{(L-x)^2}{2I_{z3}}\right]dx\Bigg\} \\
&\Bigg\{\int_0^a \left[\frac{1+\nu}{A_{sx1}} + \frac{x^2}{2I_{z1}}\right]dx \\
&+\int_a^{L-c} \left[\frac{1+\nu}{A_{sx2}} + \frac{x^2}{2I_{z2}}\right]dx \\
&+\int_{L-c}^L \left[\frac{1+\nu}{A_{sx3}} + \frac{x^2}{2I_{z3}}\right]dx\Bigg\} \\
&-\Bigg\{(L-s)\int_0^s \left[\frac{1+\nu}{A_{sx1}} + \frac{x^2}{2I_{z1}}\right]dx \\
&-s\int_s^a \left[\frac{1+\nu}{A_{sx1}} - \frac{(L-x)x}{2I_{z1}}\right]dx \\
&-s\int_a^{L-c} \left[\frac{1+\nu}{A_{sx2}} - \frac{(L-x)x}{2I_{z2}}\right]dx \\
&-s\int_{L-c}^L \left[\frac{1+\nu}{A_{sx3}} - \frac{(L-x)x}{2I_{z3}}\right]dx\Bigg\} \\
&\Bigg\{\int_0^a \left[\frac{1+\nu}{A_{sx1}} - \frac{(L-x)x}{2I_{z1}}\right]dx \\
&+\int_a^{L-c} \left[\frac{1+\nu}{A_{sx2}} - \frac{(L-x)x}{2I_{z2}}\right]dx \\
&+\int_{L-c}^L \left[\frac{1+\nu}{A_{sx3}} - \frac{(L-x)x}{2I_{z3}}\right]dx\Bigg\}\Bigg] / \\
\Bigg[\Bigg\{&\int_0^a \left[\frac{1+\nu}{A_{sx1}} - \frac{(L-x)x}{2I_{z1}}\right]dx \\
&+\int_a^{L-c} \left[\frac{1+\nu}{A_{sx2}} - \frac{(L-x)x}{2I_{z2}}\right]dx \\
&+\int_{L-c}^L \left[\frac{1+\nu}{A_{sx3}} - \frac{(L-x)x}{2I_{z3}}\right]dx\Bigg\}^2 \\
&-\Bigg\{\int_0^a \left[\frac{1+\nu}{A_{sx1}} + \frac{(L-x)^2}{2I_{z1}}\right]dx \\
&+\int_a^{L-c} \left[\frac{1+\nu}{A_{sx2}} + \frac{(L-x)^2}{2I_{z2}}\right]dx \\
&+\int_{L-c}^L \left[\frac{1+\nu}{A_{sx3}} + \frac{(L-x)^2}{2I_{z3}}\right]dx\Bigg\} \\
&\Bigg\{\int_0^a \left[\frac{1+\nu}{A_{sx1}} + \frac{x^2}{2I_{z1}}\right]dx \\
&+\int_a^{L-c} \left[\frac{1+\nu}{A_{sx2}} + \frac{x^2}{2I_{z2}}\right]dx \\
&+\int_{L-c}^L \left[\frac{1+\nu}{A_{sx3}} + \frac{x^2}{2I_{z3}}\right]dx\Bigg\}\Bigg]
\end{aligned}
\qquad (31)
$$

$$
\begin{aligned}
M_{BA} = P\Bigg[\Bigg\{&(L-s)\int_0^s \left[\frac{1+\nu}{A_{sx1}} - \frac{(L-x)x}{2I_{z1}}\right]dx \\
&-s\int_s^a \left[\frac{1+\nu}{A_{sx1}} + \frac{(L-x)^2}{2I_{z1}}\right]dx \\
&-s\int_a^{L-c} \left[\frac{1+\nu}{A_{sx2}} + \frac{(L-x)^2}{2I_{z2}}\right]dx \\
&-s\int_{L-c}^L \left[\frac{1+\nu}{A_{sx3}} + \frac{(L-x)^2}{2I_{z3}}\right]dx\Bigg\} \\
&\Bigg\{\int_0^a \left[\frac{1+\nu}{A_{sx1}} - \frac{(L-x)x}{2I_{z1}}\right]dx \\
&+\int_a^{L-c} \left[\frac{1+\nu}{A_{sx2}} - \frac{(L-x)x}{2I_{z2}}\right]dx \\
&+\int_{L-c}^L \left[\frac{1+\nu}{A_{sx3}} - \frac{(L-x)x}{2I_{z3}}\right]dx\Bigg\} \\
&-\Bigg\{(L-s)\int_0^s \left[\frac{1+\nu}{A_{sx1}} + \frac{x^2}{2I_{z1}}\right]dx \\
&-s\int_s^a \left[\frac{1+\nu}{A_{sx1}} - \frac{(L-x)x}{2I_{z1}}\right]dx \\
&-s\int_a^{L-c} \left[\frac{1+\nu}{A_{sx2}} - \frac{(L-x)x}{2I_{z2}}\right]dx \\
&-s\int_{L-c}^L \left[\frac{1+\nu}{A_{sx3}} - \frac{(L-x)x}{2I_{z3}}\right]dx\Bigg\} \\
&\Bigg\{\int_0^a \left[\frac{1+\nu}{A_{sx1}} + \frac{(L-x)^2}{2I_{z1}}\right]dx \\
&+\int_a^{L-c} \left[\frac{1+\nu}{A_{sx2}} + \frac{(L-x)^2}{2I_{z2}}\right]dx \\
&+\int_{L-c}^L \left[\frac{1+\nu}{A_{sx3}} + \frac{(L-x)^2}{2I_{z3}}\right]dx\Bigg\}\Bigg] / \\
\Bigg[\Bigg\{&\int_0^a \left[\frac{1+\nu}{A_{sx1}} - \frac{(L-x)x}{2I_{z1}}\right]dx \\
&+\int_a^{L-c} \left[\frac{1+\nu}{A_{sx2}} - \frac{(L-x)x}{2I_{z2}}\right]dx \\
&+\int_{L-c}^L \left[\frac{1+\nu}{A_{sx3}} - \frac{(L-x)x}{2I_{z3}}\right]dx\Bigg\}^2 \\
&-\Bigg\{\int_0^a \left[\frac{1+\nu}{A_{sx1}} + \frac{(L-x)^2}{2I_{z1}}\right]dx \\
&+\int_a^{L-c} \left[\frac{1+\nu}{A_{sx2}} + \frac{(L-x)^2}{2I_{z2}}\right]dx \\
&+\int_{L-c}^L \left[\frac{1+\nu}{A_{sx3}} + \frac{(L-x)^2}{2I_{z3}}\right]dx\Bigg\} \\
&\Bigg\{\int_0^a \left[\frac{1+\nu}{A_{sx1}} + \frac{x^2}{2I_{z1}}\right]dx \\
&+\int_a^{L-c} \left[\frac{1+\nu}{A_{sx2}} + \frac{x^2}{2I_{z2}}\right]dx \\
&+\int_{L-c}^L \left[\frac{1+\nu}{A_{sx3}} + \frac{x^2}{2I_{z3}}\right]dx\Bigg\}\Bigg]
\end{aligned}
\qquad (32)
$$

Eqs. (33)-(34) show the fixed-end moments, when the concentrated load "*P*" is found $a \leq x \leq L - c$

$$
\begin{aligned}
M_{AB} = P\Bigg[\Bigg\{&(L-s)\int_0^a\left[\frac{1+\nu}{A_{sx1}}-\frac{(L-x)x}{2I_{z1}}\right]dx\\
&+(L-s)\int_a^s\left[\frac{1+\nu}{A_{sx2}}-\frac{(L-x)x}{2I_{z2}}\right]dx\\
&-s\int_s^{L-c}\left[\frac{1+\nu}{A_{sx2}}+\frac{(L-x)^2}{2I_{z2}}\right]dx\\
&-s\int_{L-c}^{L}\left[\frac{1+\nu}{A_{sx3}}+\frac{(L-x)^2}{2I_{z3}}\right]dx\Bigg\}\\
&\Bigg\{\int_0^a\left[\frac{1+\nu}{A_{sx1}}+\frac{x^2}{2I_{z1}}\right]dx\\
&+\int_a^{L-c}\left[\frac{1+\nu}{A_{sx2}}+\frac{x^2}{2I_{z2}}\right]dx\\
&+\int_{L-c}^{L}\left[\frac{1+\nu}{A_{sx3}}+\frac{x^2}{2I_{z3}}\right]dx\Bigg\}\\
&-\Bigg\{(L-s)\int_0^a\left[\frac{1+\nu}{A_{sx1}}+\frac{x^2}{2I_{z1}}\right]dx\\
&+(L-s)\int_a^s\left[\frac{1+\nu}{A_{sx2}}+\frac{x^2}{2I_{z2}}\right]dx\\
&-s\int_s^{L-c}\left[\frac{1+\nu}{A_{sx2}}-\frac{(L-x)x}{2I_{z2}}\right]dx\\
&-s\int_{L-c}^{L}\left[\frac{1+\nu}{A_{sx3}}-\frac{(L-x)x}{2I_{z3}}\right]dx\Bigg\}\\
&\Bigg\{\int_0^a\left[\frac{1+\nu}{A_{sx1}}-\frac{(L-x)x}{2I_{z1}}\right]dx\\
&+\int_a^{L-c}\left[\frac{1+\nu}{A_{sx2}}-\frac{(L-x)x}{2I_{z2}}\right]dx\\
&+\int_{L-c}^{L}\left[\frac{1+\nu}{A_{sx3}}-\frac{(L-x)x}{2I_{z3}}\right]dx\Bigg\}\Bigg]\Bigg/\\
&\Bigg[\Bigg\{\int_0^a\left[\frac{1+\nu}{A_{sx1}}-\frac{(L-x)x}{2I_{z1}}\right]dx\\
&+\int_a^{L-c}\left[\frac{1+\nu}{A_{sx2}}-\frac{(L-x)x}{2I_{z2}}\right]dx\\
&+\int_{L-c}^{L}\left[\frac{1+\nu}{A_{sx3}}-\frac{(L-x)x}{2I_{z3}}\right]dx\Bigg\}^2\\
&-\Bigg\{\int_0^a\left[\frac{1+\nu}{A_{sx1}}+\frac{(L-x)^2}{2I_{z1}}\right]dx\\
&+\int_a^{L-c}\left[\frac{1+\nu}{A_{sx2}}+\frac{(L-x)^2}{2I_{z2}}\right]dx\\
&+\int_{L-c}^{L}\left[\frac{1+\nu}{A_{sx3}}+\frac{(L-x)^2}{2I_{z3}}\right]dx\Bigg\}\\
&\Bigg\{\int_0^a\left[\frac{1+\nu}{A_{sx1}}+\frac{x^2}{2I_{z1}}\right]dx\\
&+\int_a^{L-c}\left[\frac{1+\nu}{A_{sx2}}+\frac{x^2}{2I_{z2}}\right]dx\\
&+\int_{L-c}^{L}\left[\frac{1+\nu}{A_{sx3}}+\frac{x^2}{2I_{z3}}\right]dx\Bigg\}\Bigg]
\end{aligned}
\qquad (33)
$$

$$
\begin{aligned}
M_{BA} = P\Bigg[\Bigg\{&(L-s)\int_0^a\left[\frac{1+\nu}{A_{sx1}}-\frac{(L-x)x}{2I_{z1}}\right]dx\\
&+(L-s)\int_a^s\left[\frac{1+\nu}{A_{sx2}}-\frac{(L-x)x}{2I_{z2}}\right]dx\\
&-s\int_s^{L-c}\left[\frac{1+\nu}{A_{sx2}}+\frac{(L-x)^2}{2I_{z2}}\right]dx\\
&-s\int_{L-c}^{L}\left[\frac{1+\nu}{A_{sx3}}+\frac{(L-x)^2}{2I_{z3}}\right]dx\Bigg\}\\
&\Bigg\{\int_0^a\left[\frac{1+\nu}{A_{sx1}}-\frac{(L-x)x}{2I_{z1}}\right]dx\\
&+\int_a^{L-c}\left[\frac{1+\nu}{A_{sx2}}-\frac{(L-x)x}{2I_{z2}}\right]dx\\
&+\int_{L-c}^{L}\left[\frac{1+\nu}{A_{sx3}}-\frac{(L-x)x}{2I_{z3}}\right]dx\Bigg\}\\
&-\Bigg\{(L-s)\int_0^a\left[\frac{1+\nu}{A_{sx1}}+\frac{x^2}{2I_{z1}}\right]dx\\
&+(L-s)\int_a^s\left[\frac{1+\nu}{A_{sx2}}+\frac{x^2}{2I_{z2}}\right]dx\\
&-s\int_s^{L-c}\left[\frac{1+\nu}{A_{sx2}}-\frac{(L-x)x}{2I_{z2}}\right]dx\\
&-s\int_{L-c}^{L}\left[\frac{1+\nu}{A_{sx3}}-\frac{(L-x)x}{2I_{z3}}\right]dx\Bigg\}\\
&\Bigg\{\int_0^a\left[\frac{1+\nu}{A_{sx1}}+\frac{(L-x)^2}{2I_{z1}}\right]dx\\
&+\int_a^{L-c}\left[\frac{1+\nu}{A_{sx2}}+\frac{(L-x)^2}{2I_{z2}}\right]dx\\
&+\int_{L-c}^{L}\left[\frac{1+\nu}{A_{sx3}}+\frac{(L-x)^2}{2I_{z3}}\right]dx\Bigg\}\Bigg]\Bigg/\\
&\Bigg[\Bigg\{\int_0^a\left[\frac{1+\nu}{A_{sx1}}-\frac{(L-x)x}{2I_{z1}}\right]dx\\
&+\int_a^{L-c}\left[\frac{1+\nu}{A_{sx2}}-\frac{(L-x)x}{2I_{z2}}\right]dx\\
&+\int_{L-c}^{L}\left[\frac{1+\nu}{A_{sx3}}-\frac{(L-x)x}{2I_{z3}}\right]dx\Bigg\}^2\\
&-\Bigg\{\int_0^a\left[\frac{1+\nu}{A_{sx1}}+\frac{(L-x)^2}{2I_{z1}}\right]dx\\
&+\int_a^{L-c}\left[\frac{1+\nu}{A_{sx2}}+\frac{(L-x)^2}{2I_{z2}}\right]dx\\
&+\int_{L-c}^{L}\left[\frac{1+\nu}{A_{sx3}}+\frac{(L-x)^2}{2I_{z3}}\right]dx\Bigg\}\\
&\Bigg\{\int_0^a\left[\frac{1+\nu}{A_{sx1}}+\frac{x^2}{2I_{z1}}\right]dx\\
&+\int_a^{L-c}\left[\frac{1+\nu}{A_{sx2}}+\frac{x^2}{2I_{z2}}\right]dx\\
&+\int_{L-c}^{L}\left[\frac{1+\nu}{A_{sx3}}+\frac{x^2}{2I_{z3}}\right]dx\Bigg\}\Bigg]
\end{aligned}
\qquad (34)
$$

Eqs. (35)-(36) present the fixed-end moments, when the concentrated load “$P$” is placed $L - c \leq x \leq L$

$$
\begin{aligned}
M_{BA} = P\Bigg[&\Bigg\{(L-s)\int_0^a\left[\frac{1+\nu}{A_{sx1}}-\frac{(L-x)x}{2I_{z1}}\right]dx\\
&+(L-s)\int_a^{L-c}\left[\frac{1+\nu}{A_{sx2}}-\frac{(L-x)x}{2I_{z2}}\right]dx\\
&+(L-s)\int_{L-c}^{s}\left[\frac{1+\nu}{A_{sx3}}-\frac{(L-x)x}{2I_{z3}}\right]dx\\
&-s\int_s^L\left[\frac{1+\nu}{A_{sx3}}+\frac{(L-x)^2}{2I_{z3}}\right]dx\Bigg\}\\
&\Bigg\{\int_0^a\left[\frac{1+\nu}{A_{sx1}}+\frac{x^2}{2I_{z1}}\right]dx\\
&+\int_a^{L-c}\left[\frac{1+\nu}{A_{sx2}}+\frac{x^2}{2I_{z2}}\right]dx\\
&+\int_{L-c}^{L}\left[\frac{1+\nu}{A_{sx3}}+\frac{x^2}{2I_{z3}}\right]dx\Bigg\}\\
&-\Bigg\{(L-s)\int_0^a\left[\frac{1+\nu}{A_{sx1}}+\frac{x^2}{2I_{z1}}\right]dx\\
&+(L-s)\int_a^{L-c}\left[\frac{1+\nu}{A_{sx2}}+\frac{x^2}{2I_{z2}}\right]dx\\
&+(L-s)\int_{L-c}^{s}\left[\frac{1+\nu}{A_{sx3}}+\frac{x^2}{2I_{z3}}\right]dx\\
&-s\int_s^L\left[\frac{1+\nu}{A_{sx3}}-\frac{(L-x)x}{2I_{z3}}\right]dx\Bigg\}\\
&\Bigg\{\int_0^a\left[\frac{1+\nu}{A_{sx1}}-\frac{(L-x)x}{2I_{z1}}\right]dx\\
&+\int_a^{L-c}\left[\frac{1+\nu}{A_{sx2}}-\frac{(L-x)x}{2I_{z2}}\right]dx\\
&+\int_{L-c}^{L}\left[\frac{1+\nu}{A_{sx3}}+\frac{(L-x)^2}{2I_{z3}}\right]dx\Bigg\}\Bigg]\Bigg/\\
\Bigg[&\Bigg\{\int_0^a\left[\frac{1+\nu}{A_{sx1}}-\frac{(L-x)x}{2I_{z1}}\right]dx\\
&+\int_a^{L-c}\left[\frac{1+\nu}{A_{sx2}}-\frac{(L-x)x}{2I_{z2}}\right]dx\\
&+\int_{L-c}^{L}\left[\frac{1+\nu}{A_{sx3}}-\frac{(L-x)x}{2I_{z3}}\right]dx\Bigg\}^2\\
&-\Bigg\{\int_0^a\left[\frac{1+\nu}{A_{sx1}}+\frac{(L-x)^2}{2I_{z1}}\right]dx\\
&+\int_a^{L-c}\left[\frac{1+\nu}{A_{sx2}}+\frac{(L-x)^2}{2I_{z2}}\right]dx\\
&+\int_{L-c}^{L}\left[\frac{1+\nu}{A_{sx3}}+\frac{(L-x)^2}{2I_{z3}}\right]dx\Bigg\}\\
&\Bigg\{\int_0^a\left[\frac{1+\nu}{A_{sx1}}+\frac{x^2}{2I_{z1}}\right]dx\\
&+\int_a^{L-c}\left[\frac{1+\nu}{A_{sx2}}+\frac{x^2}{2I_{z2}}\right]dx\\
&+\int_{L-c}^{L}\left[\frac{1+\nu}{A_{sx3}}+\frac{x^2}{2I_{z3}}\right]dx\Bigg\}\Bigg]
\end{aligned}
\tag{35}
$$

$$
\begin{aligned}
M_{BA} = P\Bigg[&\Bigg\{(L-s)\int_0^a\left[\frac{1+\nu}{A_{sx1}}-\frac{(L-x)x}{2I_{z1}}\right]dx\\
&+(L-s)\int_a^{L-c}\left[\frac{1+\nu}{A_{sx2}}-\frac{(L-x)x}{2I_{z2}}\right]dx\\
&+(L-s)\int_{L-c}^{s}\left[\frac{1+\nu}{A_{sx3}}-\frac{(L-x)x}{2I_{z3}}\right]dx\\
&-s\int_s^L\left[\frac{1+\nu}{A_{sx3}}+\frac{(L-x)^2}{2I_{z3}}\right]dx\Bigg\}\\
&\Bigg\{\int_0^a\left[\frac{1+\nu}{A_{sx1}}-\frac{(L-x)x}{2I_{z1}}\right]dx\\
&+\int_a^{L-c}\left[\frac{1+\nu}{A_{sx2}}-\frac{(L-x)x}{2I_{z2}}\right]dx\\
&+\int_{L-c}^{L}\left[\frac{1+\nu}{A_{sx3}}-\frac{(L-x)x}{2I_{z3}}\right]dx\Bigg\}\\
&-\Bigg\{(L-s)\int_0^a\left[\frac{1+\nu}{A_{sx1}}+\frac{x^2}{2I_{z1}}\right]dx\\
&+(L-s)\int_a^{L-c}\left[\frac{1+\nu}{A_{sx2}}+\frac{x^2}{2I_{z2}}\right]dx\\
&-(L-s)\int_{L-c}^{s}\left[\frac{1+\nu}{A_{sx3}}+\frac{x^2}{2I_{z3}}\right]dx\\
&-s\int_s^L\left[\frac{1+\nu}{A_{sx3}}-\frac{(L-x)x}{2I_{z3}}\right]dx\Bigg\}\\
&\Bigg\{\int_0^a\left[\frac{1+\nu}{A_{sx1}}+\frac{(L-x)^2}{2I_{z1}}\right]dx\\
&+\int_a^{L-c}\left[\frac{1+\nu}{A_{sx2}}+\frac{(L-x)^2}{2I_{z2}}\right]dx\\
&+\int_{L-c}^{L}\left[\frac{1+\nu}{A_{sx3}}+\frac{(L-x)^2}{2I_{z3}}\right]dx\Bigg\}\Bigg]\Bigg/\\
\Bigg[&\Bigg\{\int_0^a\left[\frac{1+\nu}{A_{sx1}}-\frac{(L-x)x}{2I_{z1}}\right]dx\\
&+\int_a^{L-c}\left[\frac{1+\nu}{A_{sx2}}-\frac{(L-x)x}{2I_{z2}}\right]dx\\
&+\int_{L-c}^{L}\left[\frac{1+\nu}{A_{sx3}}-\frac{(L-x)x}{2I_{z3}}\right]dx\Bigg\}^2\\
&-\Bigg\{\int_0^a\left[\frac{1+\nu}{A_{sx1}}+\frac{(L-x)^2}{2I_{z1}}\right]dx\\
&+\int_a^{L-c}\left[\frac{1+\nu}{A_{sx2}}+\frac{(L-x)^2}{2I_{z2}}\right]dx\\
&+\int_{L-c}^{L}\left[\frac{1+\nu}{A_{sx3}}+\frac{(L-x)^2}{2I_{z3}}\right]dx\Bigg\}\\
&\Bigg\{\int_0^a\left[\frac{1+\nu}{A_{sx1}}+\frac{x^2}{2I_{z1}}\right]dx\\
&+\int_a^{L-c}\left[\frac{1+\nu}{A_{sx2}}+\frac{x^2}{2I_{z2}}\right]dx\\
&+\int_{L-c}^{L}\left[\frac{1+\nu}{A_{sx3}}+\frac{x^2}{2I_{z3}}\right]dx\Bigg\}\Bigg]
\end{aligned}
\tag{36}
$$